Study of Acoustic Emission Arising from Pure Tensile Cracks in Concrete

Hisham A. Elfergani
Faculty of Engineering
University of Benghazi, Libya
Hisham.elfergani@uob.edu.ly

Ayad A. Abdalla
Faculty of Engineering
University of Benghazi, Libya
Ayad.abdalla@uob.edu.ly

Abstract:

Cracks are a major cause of damage in concrete structures thus it is of great importance to identify the type of cracks and their distribution. This paper reports on a study of the acoustic emission (AE) from a concrete specimen under pure tensile loading in order to promote only one type of crack signal to identify the characteristics of AE signals gained from pure tensile cracks. For this purpose a bespoke concrete specimen was designed to avoid stress concentration issues and to allow observation of micro cracks. Results indicate that AE is capable of detecting and identifying tensile cracks using the RA/AF value and that tensile type cracks in concrete have relatively small RA value (less than 5 ms/v).

Key Words: Acoustic emission, monitoring, concrete, pure tensile, crack classification.

الملخص

تعتبر التشققات من الاسباب الرئيسية لتضرر و انهيار المنشآت الخرسانية مما يجعل تحديد نوع هذه التشققات و طريقة توزيعها أمراً بالغ الاهمية. في هذا البحث يتم دراسة الانبعاثات الصوتية AE الناتجة من تسليط حمل شد صافي على عينة خرسانية بهدف تحفيز ظهور نوع واحد من التشققات (تشقق شدَ) مما يسمح بدراسة, وتحديد خصائص المميزة لإشارات AE الناتجة من تشققات الشد. لهذا الغرض تم تصميم شكل العينة الخرسانية غير اعتيادية بطريقة تمنع حدوث تركز الاجهادات و تسمح في الوقت نفسه بملاحظة التشققات المجهرية. و قد بينت نتائج هذه الدراسة ان تقنية AE قادرة على استشعار و والتعرف على تشققات الشد باستخدام قيم RA/AF كما بينت النتائج ان تشققات الشد في الخرسانة تتميز بقيمة صغيرة نسبياً لـ RA (أقل من 5 ملي ثانية/فولت).

كلمات مفتاحية: الانبعاثات الصوتية، المراقبة، خرسانة، حمل شد صافي، تصنيف التشققات.

1. Introduction

Concrete is the most widely used construction material in the world today (Aïtcin, 2000), and hence among the substantial challenges which face engineers is to find the best way to detect the early stages of deterioration of the concrete structures. For this purpose, non-destructive evaluation (NDE) techniques are often applied to monitor and estimate the safety and the performance of current state of concrete structures and to help make a decision on maintenance and correction measures. Acoustic emission (AE) is one of the effective NDE techniques in investigating local damage in concrete. It can be defined as "the transient elastic waves which are generated by the rapid release of energy from localised sources within a material" (Miller et al., 2005). The release of elastic energy occurs when the material undergoes deformation. The released energy propagates through the material in all directions and is detected at the structure surface using a piezoelectric transducer (sensor). Several sensors are mounted at different positions to detect the displacement of the surface and convert it into electric signals. The strength and location of the AE source can be estimated by analysis of the resultant waveform in terms of feature data such as amplitude, energy and time of arrival of AE waveforms at each sensor. Several studies suggest that the relationship between RA values (rise time/ Amplitude) and average frequencies (counts/duration) can be used for classification of crack types (Aggelis 2011, Ohno and Ohtsu 2010, Ohtsu and Tomoda 2007, Soulioti et al 2009, Elfergani et al 2013). Shear type crack are characterised by an AE signal with low average frequency and high RA value while tensile type crack AE signal has a high average frequency and low RA value, as shown Figure 1 and Figure 2.

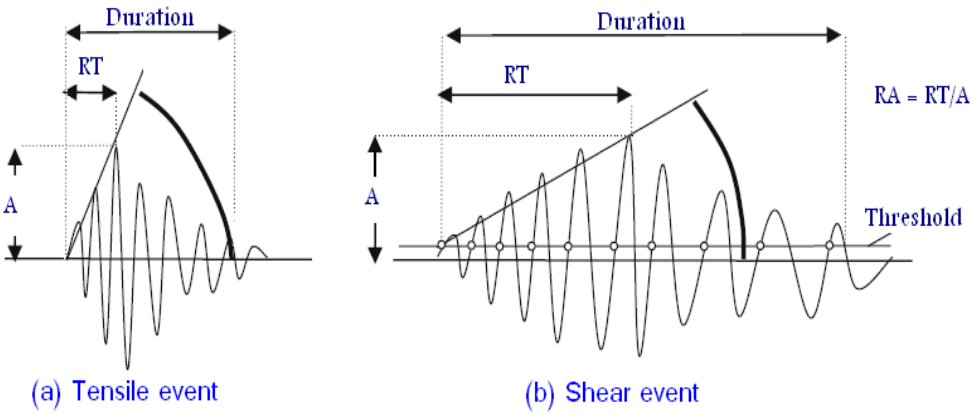

Figure **1** Typical waveforms (Soulioti et al 2009)

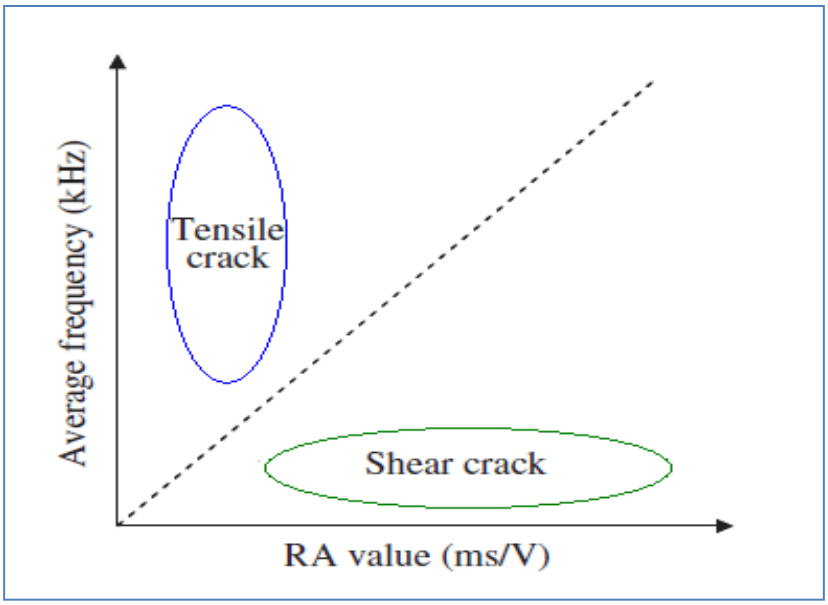

Figure 2 Crack classifications (Ohno and Ohtsu 2010)

In this paper, AE techniques are employed to identify the characteristics of AE signals gained from pure tensile cracks. Parameter analysis is used to analyse the detected AE signals and the results of the crack characteristics are discussed.

2. Experimental Procedure

2.1 Specimen preparation

The common problem when using the classic shape of concrete sample (cylinder or prism) for uniaxial tension testing is that there is a stress concentration due to a mismatch between the Young's modulus and Poisson's ratio of concrete and steel when the steel loading plates are bonded onto the specimen. To avoid this issue, notched specimens are often used. However, this practise makes it not possible to observe the formation and propagation of micro cracks as they form at a small area around the notch. In order to avoid these restrictions, the specimen shape is designed as a dog-bone a continuous transition curve such that the failure should occur in the narrow part of the specimen. This specimen geometry, Figure Figure3, ensures a uniform tensile stress field over a large area which is unaffected by the loading arrangement making it possible to observe the micro crack evolution (Benson 2003).

Figure3 Concrete tensile specimen

The dog-bone type shape specimen has 740 mm length (500 mm of which is the transition spline), 100 mm width at the specimen's centre which increases gradually to 200 mm at the end of the spline and 35 mm thickness. The concrete consists of one part cement to not more than three parts aggregate (by weight). Portland cement CEM II/BV32.5R was used and the specimen was water cured for 28 days (Elfergani et al 2011).

A combination of bonded plates and pinned plates was used to grip the specimen. This type of grip was adopted because it had proved effective previously (Benson 2003). A pair of plates was bonded, at both ends, using a commercial bonding agent (Sika bonding -Sikadur 31) as shown in Figure 4. In order to ensure that the adhesive had achieved its full strength, the specimens were left in the jig for 24 hours. These plates were pinned to a top plate which was attached to a coupling with a pin.

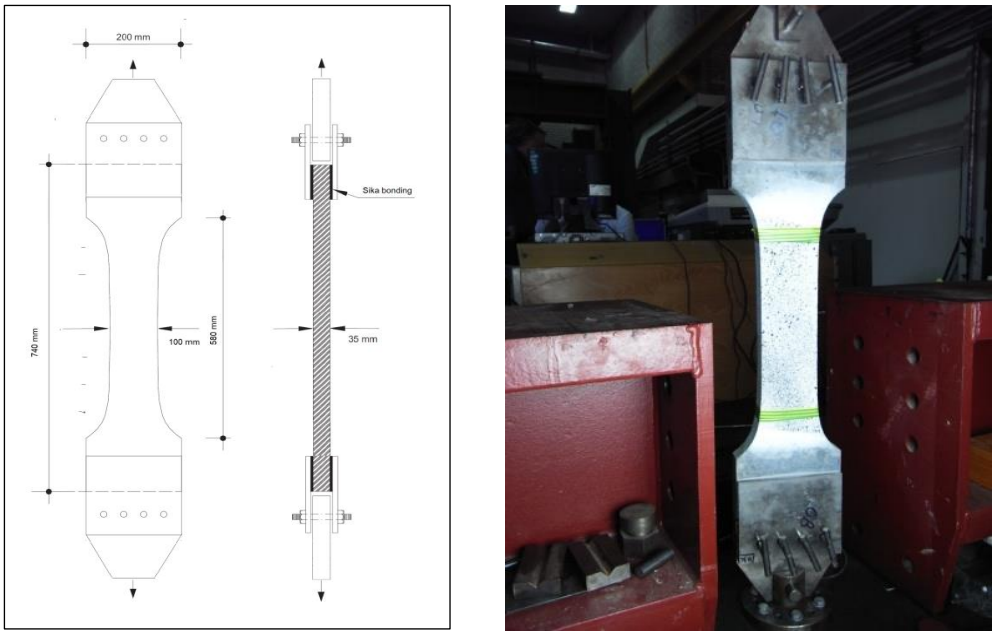

Figure 4 Tensile specimen geometry and loading arrangement

2.2 Test set-up

A coupling was fixed on to a thick steel plate mounted on two I-beams. The top coupling was connected with the load cell attached to the actuator in the testing machine.

Two AE sensors (R3I – resonant frequency 30 kHz) were mounted to the centre of the mortar surface. The AE sensor was mounted using silicon sealant and fixed by adhesive tape. The AE systems hardware was set-up with threshold level of 40 dB and the sensitivity of the mounted sensors was checked by using the Hsu-Neilson source (Hsu 1979). The specimen was loaded gradually in tension and the AE system recorded the hits up to final failure. Figure 5 shows photographs of the loading arrangement. Time of Arrival (TOA) method (Miller and Mclntire 1987 and Rindorf 1981) was used to locate signals. This method is the simplest method for source location and is based on the arrival time of the source event at two or more sensors. When using this method, the wave velocity of the signals that propagate through the material needs to be determined.

Figure 5 Photograph of concrete specimen in the test machine

3. Results and Discussion

Two loading scenarios were used in the current study. In Scenario I, the load was applied in two stages; in the first stage a rate of 0.002 mm/s was applied from the beginning until 310 sec and in the second stage the rate was decreased to 0.001mm/s until the failure in order to control the rate of crack growth prior to failure. While in Scenario II the applied load was started with small rate of 0.001 mm/sin the first stage until 250 sec then increased 0.002 mm/s in the second stage.

3.1 Scenario I

The variation of applied load against time is shown in Figure **6**. All the detected and located signals above a minimum amplitude of 45 dB detected by the two sensors for the whole duration of the tensile test are shown in Figure 7 as signal amplitude against time, while Figure 8 displays the same data set but this time as energy against time. The detected energy is attributed to a number of sources; micro and macro tensile cracking and load machine noise and specimen failure. It can be seen that the first hits occur before 100 seconds which the applied load reaches 2kN and the final failure occurred at 12.74 kN (543 sec).

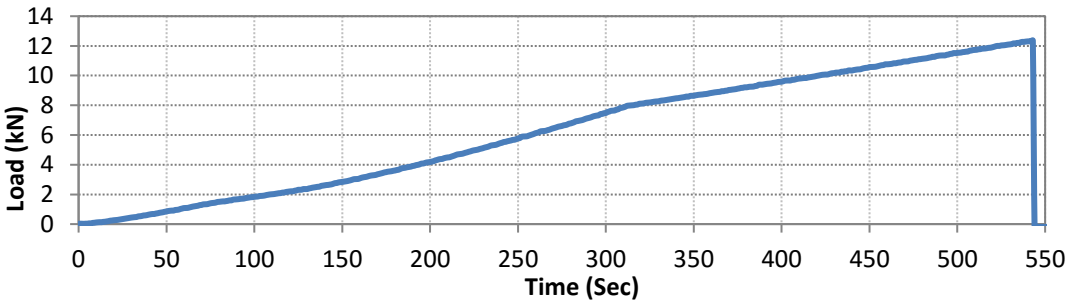

Figure 6 Applied loads vs. Time

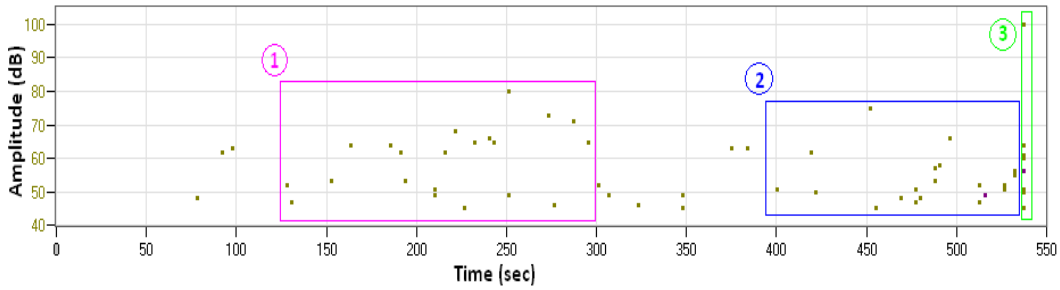

Figure 7 Amplitude vs. Time

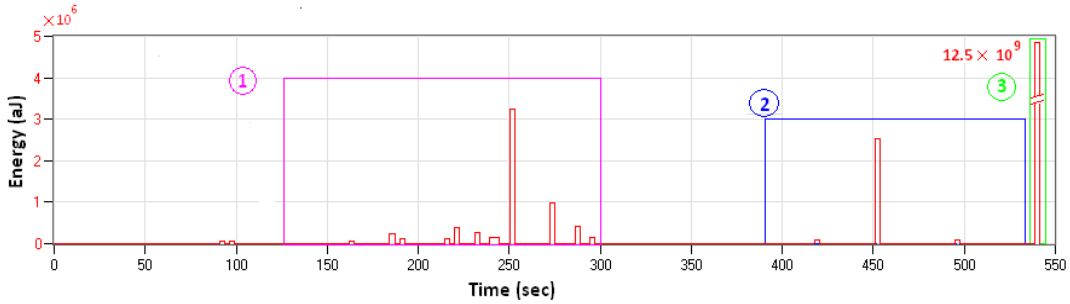

Figure 8 Absolute energy vs. Time

It can be seen that in Figures 7 and 8 there are three significant periods of AE. Period 1 may be attributed to the energy release from the loading machine because no evidence of micro cracks was visually observed at this time. The emission in period 2 is attributed to micro crack and dislocation in the specimen from visual observation. It should be noted that period 1 has slightly more AE activity but this is attributed to higher load rate during that period. The highest energy and highest amplitude in a short time in period 3 corresponds to the formation of a tensile macro cracks and specimen failure.

Figures 9 (a, b and c) show the relationship between the RA value and average frequency of the three periods. Figure 9 (a) shows the relationship between RA value and AF for period 1 which is associated with the early period of the test before any crack occurred. It can be seen that most of the data points have wide RA value (RA values 0-25 ms/v) and with low AF values (less than 20 kHz). Figure 9 (b) shows the relationship between RA value and AF for period 2 associated with the period directly before failure. It can be seen that there is a tendency for the data points have a narrower range of RA values with higher AF values. However Figure 9 (c) represents the relationship between RA value and AF for period 3 the failure period. It can be noted that in this period the most of the data points have various AF and low RA value (less than 5 ms/v).

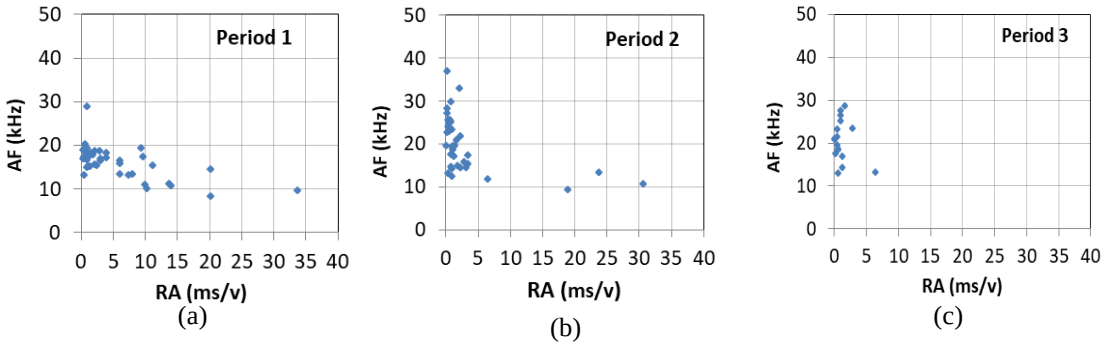

Figure 9 Relation between the RA value and average frequency of (a) Period 1, (b) Period 2 and (c) Period 3

The location of signals with minimum amplitude of 45 dB for the whole period of the test is shown in Figure 10 as signal amplitude vs. position and Figure 11 displays the same data set but this time as energy vs. position. Figure 12 is a photograph of the specimen after the end of the test, showing the crack location and crack shape.

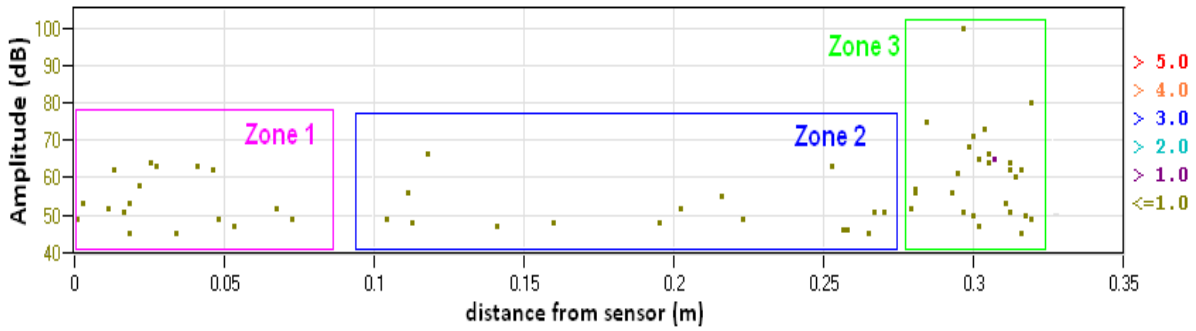

Figure 10 Amplitude vs. liner location vs. Hits

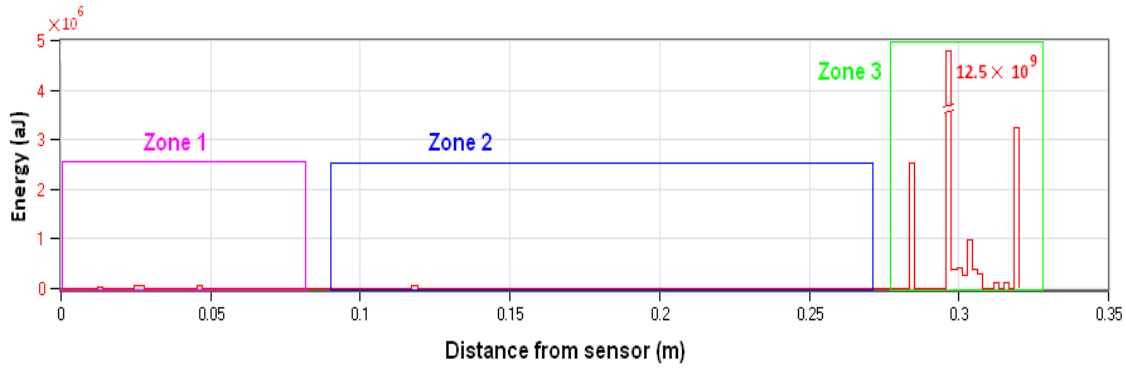

Figure 11 Absolute energy vs. liner location

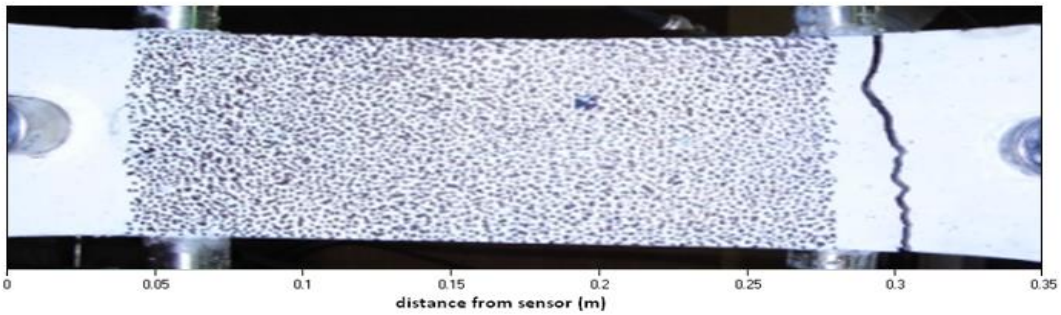

Figure 12 Photos of specimen after failure

It can be noted that there are three zones in Figure 10 and 11. In zone 1 and 2 there are a small number of hits, low amplitude and with very low energy. By comparing with Figure 12 these zones are corresponding to areas with no crack. Zone 3 has higher hits concentration, high amplitude and highest energy and coincides with the location of the crack which was visibly observed post-test as shown in Figure 12 .

Figure 13 (a, b and c) show the AF vs. RA values for the different three regions. Figure13 (a and b) show the AF vs. RA for zones 1 and 2 which are associated with the no crack regions. It can be noted that in these areas the RA value have a wide distribution (RA values 0-35 ms/v). Figure 13 (c) shows the relationship between RA value and AF of zone 3 associated with the tensile crack type region. It can be seen that the most of data points have various AF and low RA value (less than 3 ms/v).

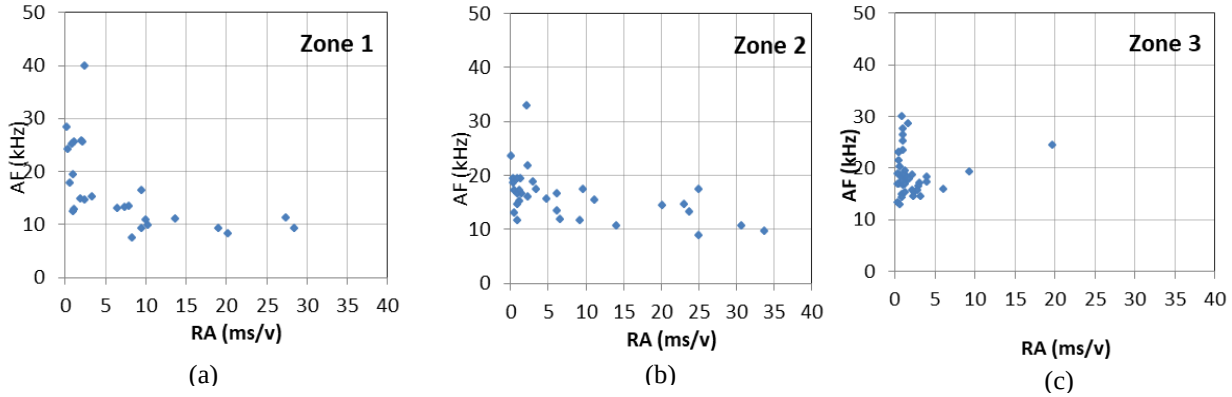

(a) (b) (c)

Figure 13 Relation between the RA value and average frequency of (a) zone1, (b) zone2 and (c) zone3

3.2 Scenario II

Similar behaviour was observed in Scenario II. The variation of load applied against time is shown in Figure 14 .

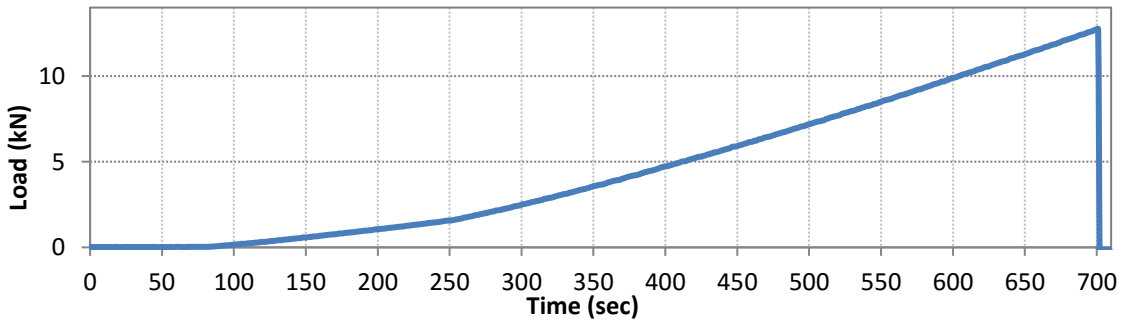

Figure 14 Applied loads vs. Time

All the detected and located signals above a minimum amplitude 45 dB detected by two sensors for the whole duration of tensile test and continuous monitoring are shown in Figure 15 as signal amplitude against time, while Figure 16 displays the same data set but this time as energy against time. The detected energy is attributed to a number of sources; macro cracking, load machine noise and specimen failure.

It can be seen that the first hits occur before 300 seconds when the applied load reaches 2kN and the final failure occurred at 12.74 kN (695 sec).

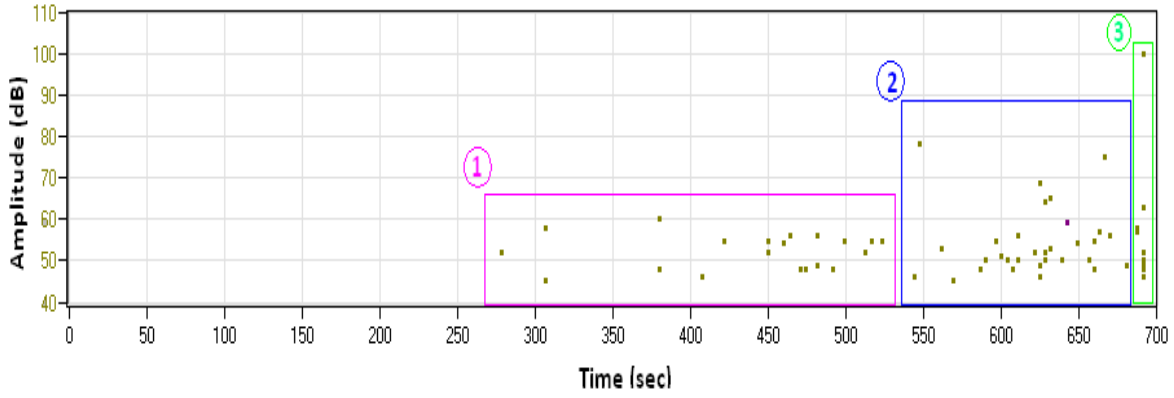

Figure 15 Amplitude vs. Time

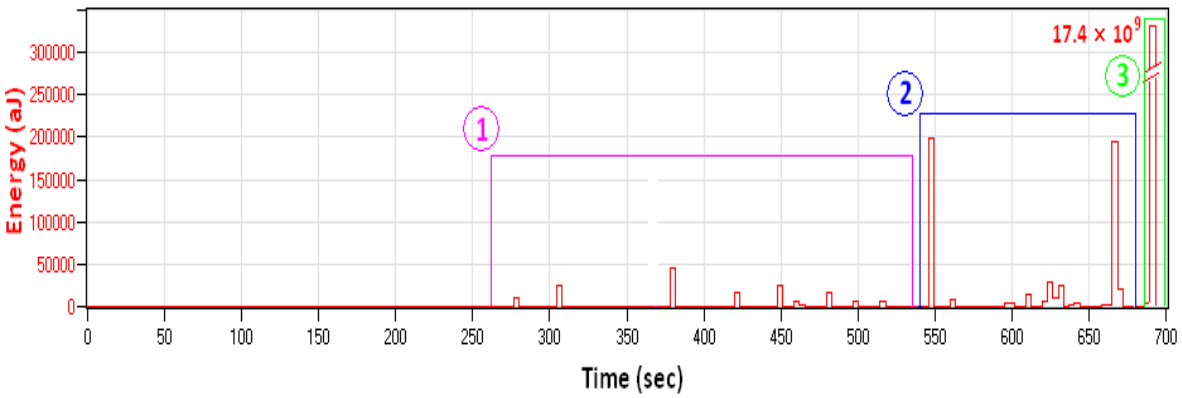

Figure 16 Absolute energy vs. Time

Figures 17 (a, b and d) show the relation between the RA value and average frequency of three periods. Figure 17(a) shows the relation of RA value and AF value in period 1 associated with the early period of the test before any crack occurred. It can be seen that the most of data points have broad RA value (RA values 0-25 ms/v) and with low AF values (less than 20 kHz) and

Figure 17 (b) shows the relationship between RA value and AF in period 2 associated with the period directly before failure.

It can also be seen that there is a tendency for the data points to have narrower RA values and with higher AF values. Figure 17 (c) represents period 3 which is the failure period. It can be noted that in this period that most of the data points have various AF and very low RA values (less than 5 ms/v) which is termed a "vertical trend". Therefore, based on Figure 2 this indicates that the type of the crack is pure tensile.

It can be seen that the results in Figures 17 (a, b and c) exhibit very similar behaviour as those in Figures 9 (a, b and c) in Scenario I.

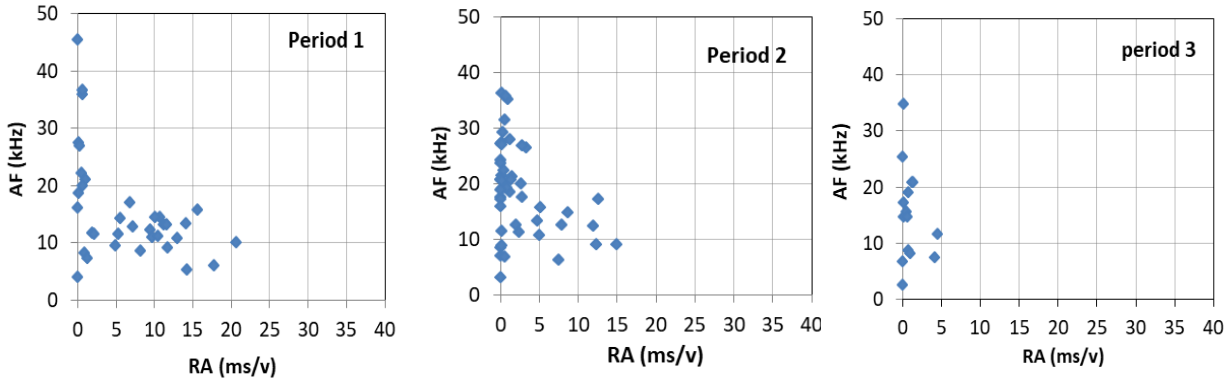

(a) (b) (c)

Figure 17 Relation between the RA value and average frequency of period 1, (b) period 2 and (c) period 3

4. Conclusion

In the present work an experimental investigation to identify tensile crack in concrete using AE is conducted. A specially designed concrete sample is subjected to pure tensile load until failure. Two different loading configurations were used in this study. It was found that tensile cracks in concrete can be identified and distinguished from other sources using the RA/AF value and that tensile type crack have small RA value (less than 5 ms/v).

References

- Aggelis D. ,(2011), Classification of cracking mode in concrete by acoustic emission parameters, Mechanics Research Communications, 38, 153-157.
- Aïtcin P.C., (2000), Cements of yesterday and today: concrete of tomorrow. Cement and Concrete research, 30(9), 1349-1359,.
- Benson, S.D.P., (2000), PhD Thesis, CARDIFRC®: development and constitutive behaviour, Cardiff School of Engineering, University of Wales, Cardiff.
- Elfergani H., Pullin R., Holford K, (2011), Acoustic emission analysis of prestressed concrete structures, Journal of Physics: Conference Series 305 (1), 012076.
- Elfergani H., Pullin R., Holford K, (2013), Damage assessment of corrosion in prestressed concrete by acoustic emission, *Construction & Building Materials Journal 40* pages 925–933.
- Hsu N.N. & Breckenbridge, F.R., (1979), Characterization and Calibration of Acoustic Emission Sensors, Materials Evaluation 39, 60-68.
- Miller R., Hill R. & Moore, P.O., (2005), Non-destructive Testing Handbook Vol. 6, 3rd Ed., Acoustic Emission Testing, American Society for Nondestructive Testing. Inc., USA.
- Miller R.K. & Mclntire, P., (1987), Acoustic Emission Testing. NDT Handbook Vol 5, second edition, American Society for Nondestructive Testing, 151.
- Rindorf H. J., (1981), Acoustic emission source location in theory and in practice, Bruel and Kjaer Technical Review, 2, pp. 3-44.
- Ohno K. & Ohtsu, M.,(2010), Crack classification in concrete based on acoustic emission, Construction and Building Materials, 24, 2339-2346.
- Ohtsu M. & Tomoda, Y. (2007), Corrosion process in reinforced concrete identified by acoustic emission, Materials Transactions, Vol 48, 1184 – 1189.
- Soulioti D., Barkoula N. M., Paipetis A., Matikas T.E, Shiotani T. & Aggelis, D.G., (2009), Acoustic emission behaviour of steel fibre reinforced concrete under bending, Construction and Building Materials, 23. 3532-3536.